Transient Performance Analysis of a Multicorrelator Signal Quality Monitor

R. Eric Phelts, Alexander Mitelman, Sam Pullen, Dennis Akos, Per Enge

Department of Aeronautics and Astronautics
Stanford University, Stanford, California

BIOGRAPHY

R. Eric Phelts is a Ph.D. candidate in the Department of Aeronautics and Astronautics at Stanford University. He received his B.S. in Mechanical Engineering from Georgia Institute of Technology in 1995, and his M.S. in Mechanical Engineering from Stanford University in 1997. His research involves multipath mitigation techniques and satellite signal anomalies.

Alexander Mitelman is a Ph.D. candidate in the Department of Electrical Engineering at Stanford University. As a member of the GPS Laboratory, his research is focused on local area differential GPS design, signal analysis, and applications. Mr. Mitelman received his S.B. in Electrical Engineering from the Massachusetts Institute of Technology in 1993 and his M.S. in Electrical Engineering from Stanford University in 1995.

Sam Pullen received his S.B. from MIT and his Masters and Ph.D. in Aeronautics and Astronautics from Stanford University, where he is now the Technical Manager of Stanford's Local Area Augmentation System project. His research focuses on system design and integrity algorithms for both the Local Area and Wide Area Augmentation Systems. He was the recipient of the ION Early Achievement Award in 1999.

Dennis M. Akos completed the Ph.D. degree in Electrical Engineering at Ohio University conducting his graduate research within the Avionics Engineering Center. After completing his graduation he has served as a faculty member with Luleå Technical University, Sweden and is currently a research associate with the GPS Laboratory at Stanford University. His research interests include GPS/CDMA receiver architectures, RF design, and software radios.

Per Enge is an Associate Professor of Aeronautics and Astronautics at Stanford University, where he has been on the faculty since 1992. His research deals with differential operation of GPS for landing aircraft. Previously, he was an Associate Professor of Electrical Engineering at Worchester Polytechnic Institute.

ABSTRACT

The ability to monitor and detect problematic distortions in the received GPS-SPS signal is a task of critical importance. Detection of these satellite signal anomalies or "evil waveforms" (EWFs) can be accomplished using detailed monitoring of the correlation peak. Using the proposed "2nd-Order Step" (2OS) Threat Model for evil waveforms, previous analysis has shown that, in steady state, monitoring sufficient to satisfy GBAS and SBAS requirements for Category I precision approaches may be obtained from a receiver design that requires minimal modifications to existing GPS hardware. In other words, ignoring time-to-alarm requirements, it has been shown that these anomalous waveforms can be detected using a practical, multicorrelator SQM implementation—defined as SQM2b. The ability of the monitor receiver to detect hazardous evil waveforms within the time to alarm, however, is necessary to guarantee airborne users never experience hazardously misleading information.

This paper shows that, without modification, SQM2b (previously validated by steady-state analysis alone) does not promptly mitigate this integrity threat. Further, it suggests that modifying the smoothing filter for the detection metrics can slightly decrease the response time required by the monitor detect these waveforms. More significantly, leveraging the same measurements taken from SQM2b, it introduces an additional nonlinear

detection test that improves the sensitivity of the monitor to detectable anomalous waveforms. The paper presents analytical results which verify that these modifications can detect the hazardous waveforms within the 6-second time-to-alarm required by LAAS. Finally, it validates the performance of this test using experimental data taken from a real-time evil waveform-generating hardware.

INTRODUCTION

Satellite signal anomalies, or "evil waveforms" (EWFs) are caused by subtle failures on the signal generating hardware on the GPS satellite. One such failure occurred in 1993 on SV19, and reportedly caused from 2-8m vertical position errors between an avionics receiver and a (local) ground differential reference station. The nominal vertical errors—obtained without including SV19—were approximately 50cm. [1][2]

Signal quality monitoring (SQM) is needed for high-integrity GPS applications such as landing commercial aircraft. Consequently, it is an important component of GPS augmentation systems such as LAAS (Local Area Augmentation System) and WAAS (Wide Area Augmentation System). SQM attempts to detect EWFs which might degrade the navigation solution integrity and receive hazardously misleading information (HMI).

BACKGROUND: STEADY-STATE SQM PERFORMANCE

The previous SQM analysis consisted of the following primary tasks:
1. Define an appropriate threat model for the EWFs that adequately describes and bounds reasonable satellite failure modes.
2. Design a practical multicorrelator receiver implementation, and determine a set of tests to detect the hazardous anomalous waveforms in the presence of nominal noise and multipath (at all satellite elevation angles).
3. Verify that the monitor design protects all ICAO-accepted user receiver designs and is robust to variations in receiver precorrelation filters. [3]
4. Validate the threat model and detector effectiveness experimentally. [5][6]

The accepted EWF threat model is known as the "2nd-Order Step" (2OS) Threat Model. It models the anomaly as both an analog and a digital failure: 2nd-order "ringing" on the C/A code chips and a digital "lead" or "lag" of the falling edge of the C/A code chips. The following three possible failure modes exist within the 2OS Threat Model:
- Threat Model A (TM A): Digital Failure Only,
- Threat Model B (TM B): Analog Failure Only, and

- Threat Model C (TM C): Combination Analog and Digital Failure.

(The equations, derivations and parameters for each of these failure modes are provided in [1] and [4].) Figure 1 illustrates the distortions caused by one EWF formed by a combination of analog and digital failure modes.
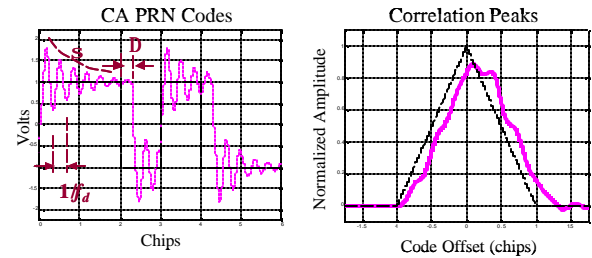

Figure 1 Example of Ideal and "Evil Waveforms" for Combination Analog and Digital Failure Modes
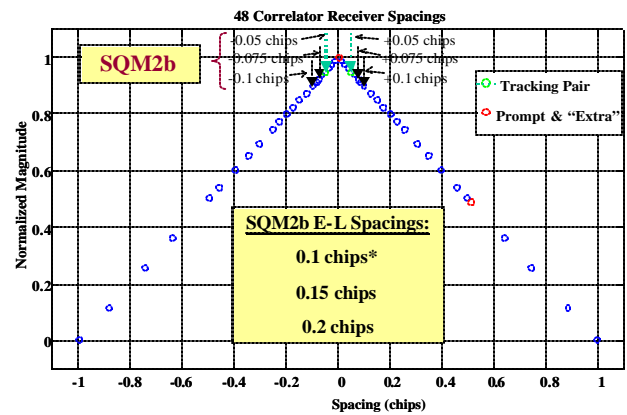

Figure 2 Monitor Receiver Correlator Configuration for SQM2b (Shown to Scale)

SQM2b refers to the monitor receiver correlator configuration designed to detect all hazardous EWFs within the 2OS threat model. This configuration places three correlators at near the top of the correlation peak—where the noise and multipath distortion is minimized. (See Figure 2.) The three spacings are 0.1, 0.15, and 0.2 chips wide; the $0.15T_c$ and $0.2T_c$ spacings are held fixed relative to the tracking pair at $0.1T_c$.

SQM2b uses two basic symmetry tests—2 Δ-tests and 9 Ratio tests—to detect anomalous correlation peak distortions. Assuming the monitor receiver is phase-locked to a signal and in-phase, I, samples from each correlator are available, a Δ-test is given as

$$\Delta_{\pm offset1, \pm offset2} \equiv \frac{\left(I_{-offset1} - I_{+offset1}\right) - \left(I_{-offset2} - I_{+offset2}\right)}{2 \cdot I_{prompt}} \quad (1)$$

where "*offset*" refers to one-half correlator spacings as measured from the Prompt correlator. An "average" Ratio test is given as

$$R_{\pm\text{offset},P} \equiv \frac{I_{-\text{offset}} + I_{+\text{offset}}}{2 \cdot I_{\text{prompt}}} \qquad (2)$$

and "single-sided" Ratio tests as

$$R_{-\text{offset},P} \equiv \frac{I_{-\text{offset}}}{I_{\text{prompt}}} \quad \text{and} \quad R_{+\text{offset},P} \equiv \frac{I_{+\text{offset}}}{I_{\text{prompt}}} \qquad (3)$$

Although the 2OS threat model presumes a satellite may have only a digital failure or only an analog failure alone, the largest user (differential) pseudorange errors (PREs) generally occur for the combination (ringing and lead/lag) failure mode. These EWFs tend to be most difficult to detect for SQM2b yet they cause relatively large PREs for the users.

The user avionics of concern fall within the ICAO-accepted receiver designs specified by tracking loop (DLL) type, precorrelation bandwidth and correlator spacing. The two tracking loop types—early-minus-late (E-L) and double-delta ($\Delta\Delta$)—have significantly different characteristic in terms of noise performance and, more importantly, multipath mitigation ability. ($\Delta\Delta$ receivers types include the Strobe Correlator [7] [8], High-resolution Correlator [9], etc.) As a result, they also can result in significantly larger differential PREs, compared to E-L receivers, from the same EWFs [3][4].
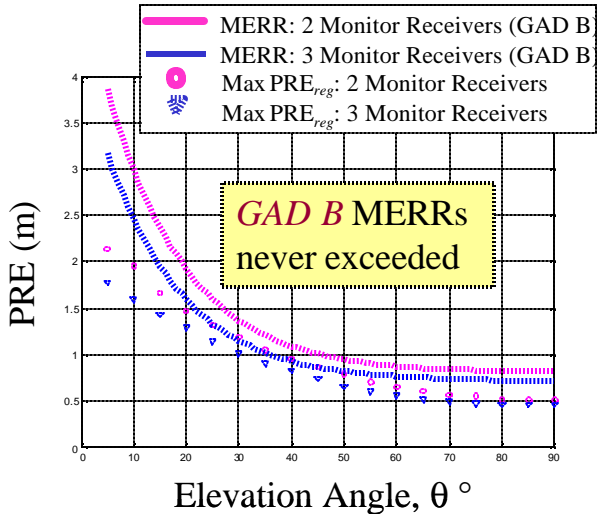

Figure 3 LAAS Cat I Steady-State SQM Performance Summary ($\Delta\Delta$ Users, Combination Analog and Digital EWF Failure Modes)

Using SQM2b to detect the waveforms within the 2OS model, the worst case PREs result from undetectable EWFs impacting $\Delta\Delta$ users. Figure 3 plots the maximum $\Delta\Delta$ PREs from these undetected waveforms versus elevation angle.

(Note that higher elevation angles generally reduce noise and multipath and permit greater detection sensitivity [4].) Figure 3 also plots two of the LAAS General Accuracy Designator B, or Maximum Error Range Residual (MERR), curves, for comparison. These indicate the LAAS Cat I maximum PRE requirements [10]. The figure implies that in steady state, SQM2b is able to protect all LAAS users from these threats. (A more complete analysis of the SQM detection problem and of the robustness of SQM2b to receiver precorrelation filter variations is given in [4].)

SQM ANALYSIS ASSUMPTIONS

The SQM analysis to date has verified that the existence of a practical multicorrelator implementation (SQM2b) capable of protecting user integrity against hazardously misleading information induced by evil waveforms. That analysis implicitly assumed, however, that the EWF failure had reached steady state. In other words, it assumed the EWF detection metrics measured by the monitor receiver and the tracking errors measured by the receivers had reached their final, steady state values. Filtering of both these observables, however, implies the transient values will, in general, differ from their steady state (i.e., maximum) values. In order to determine whether the hazardous EWFs cause HMI for airborne users, it is necessary to first make assumptions for how the satellite failure occurs. Also, the filter transient responses to that EWF failure must be modeled. If it is discovered that some EWFs cause transient SQM problems, it may become necessary to add even more sensitive detection metrics to mitigate this threat.

The transient SQM analysis assumes that any EWF failure will occur instantaneously (and persist for a long time relative to the transient responses of any measurement filters such as carrier smoothing). It further assumes that the instantaneous error resulting in the receiver can be approximated by a step function that occurs at time $t=t_{EWF}$. The amplitude of this (step) error, A_{tss}, is dependent on the observable measured by the receiver. For SQM, there are three such observables. These configuration-dependent variables include the following:

1. Reference station tracking error (i.e., differential error correction)
2. Monitor receiver SQM detection metrics (i.e., correlator value measurements)
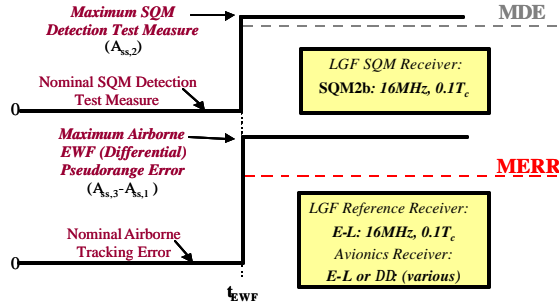3. Airborne receiver tracking errors

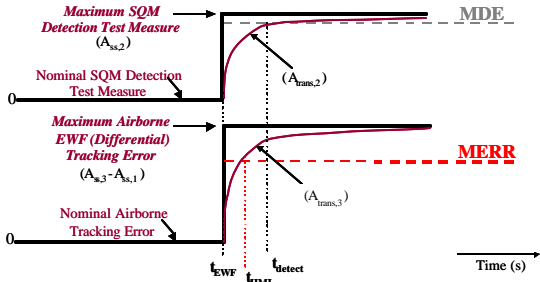**Figure 4 Steady-State SQM Problem**

Figure 5 Transient SQM Problem with 1st-Order Filter Responses

At the onset of a satellite failure, the tracking errors for the reference station and the user will asymptotically approach their (different) steady-state values, $A_{ss,1}(t)$ and $A_{ss,3}(t)$, respectively (refer to Figures 4 and 5). Simultaneously, each of the monitor receiver detection metrics will also approach their respective steady-state values. Assuming the same filter is applied to all detection metrics, the maximum, $A_{ss,2}(t)$, will correspond to the most sensitive detection test (recall that only a single metric needs to exceed its corresponding MDE for detection of an EWF).

The transient airborne error responses of hazardous EWFs will exceed their corresponding MERRs at $t = t_{HMI}$. If the EWF is detectable, this (most sensitive) test will ideally detect it at time, $t = t_{detect} \leq t_{HMI}$. Less conservatively, however, to meet the LAAS Cat I time-to-alarm requirement, t_{detect} can exceed t_{HMI} by no more than 3 seconds—one-half of the total 6-second time-to alarm requirement. This analysis assumes the LAAS Ground Facility takes a maximum of 3 seconds to detect and alert the user, and the user requires 3 seconds to receive and process the alarm message. Hence, we define TTA = 6 and TTA_{LGF} = TTA/2 = 3s. The transient performance of a monitor is satisfactory when $t_{detect} \leq t_{HMI} + TTA_{LGF}$. Otherwise, it is unsatisfactory, and the user error will correspond to time, $t = t_{detect} + TTA_{LGF}$.

FILTER RESPONSE MODELS

1st-Order Filter

The filter used to carrier-smooth pseudorange measurements, has a first-order response. Accordingly, the time domain response of a this filter is given by

$$A_{trans}(t) = A_{ss}\left(1 - e^{-t/t_c}\right) \quad t \geq 0 \qquad (4)$$

where $A_{trans}(t)$ is the transient response of the EWF-induced variation, $A_{tss}(t)$ is the maximum (i.e., steady-state) amplitude of the variation, and t_c is time constant of the filter ($t_c = 100s$ for LAAS receivers).

Figure 5 illustrates the transient SQM problem for a first-order smoothing of the detection tests (and user differential PREs). The figure shows the (fastest) transient responses of the monitor receiver for one example user receiver configuration. Note that as shown, $A_{trans,2}(t - t_{EWF})$ is the transient response resulting from a first-order filter applied to the detection metrics measurements. The maximum transient differential airborne receiver PREs, $A_{trans,3}$, are given by

$$A_{trans,3}(t - t_{EWF}) = (A_{ss,3} - A_{ss,1})\left(1 - e^{-(t-t_{EWF})/t_c}\right) \quad (5)$$

where $t > t_{EWF}$. It follows that the basic transient SQM problem (with TTA=0 seconds) reduces to a simple comparison of the normalized steady state errors according to

$$\begin{cases} \dfrac{A_{ss,3} - A_{ss,1}}{MERR(?)} > \dfrac{A_{ss,2}}{MDE(?)}, & t_{detect} > t_{HMI} \\ \text{otherwise}, & t_{detect} \leq t_{HMI} \end{cases} \qquad (6)$$

where θ is the satellite elevation angle.

Moving Average (FIR) Filter: Linear Response

Although LAAS requires that a 1st-order filter be used for carrier smoothing of the airborne and reference receiver tracking errors, the SQM metrics may be smoothed with a different filter [10]. For these, the most desirable transient response is one that has as fast a rise time as possible. This implies, however, that the filter has a smaller time constant, or rather that it has a wide bandwidth. In fact, no filtering at all would essentially provide the SQM with a response virtually as fast as the (instantaneous) EWF failure itself.

Wide-bandwidth filtering in general is not practical, since the MDEs presume a filter will adequately smooth the metrics. Recall that this smoothing is required to reduce

the nominal variations due to multipath and thermal noise. A faster filter implementation would necessarily require computation of new MDEs, which would, of course, become larger. One simple compromise is to leverage the fact that the ICAO-accepted Stanford University (SU) MDEs already assume a more conservative (i.e., faster) smoothing filter than a first-order filter [4]. The MDEs are computed using a 100-tap FIR rectangular window, or a 100-second "moving average" filter. (Each tap of this filter corresponds to one second.)
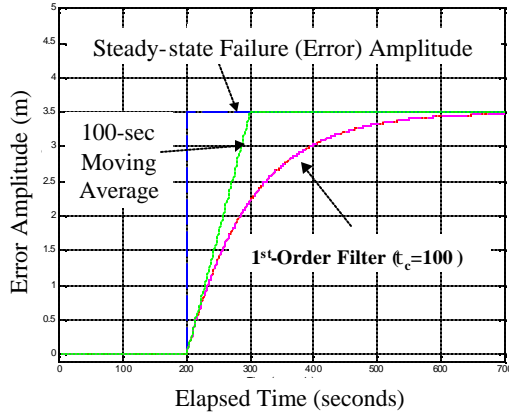
Figure 6 Comparison of 1st-Order and Moving Average (100-tap FIR) Filter Transient Responses

A comparison of the transient responses of the 1st-order filter and the moving average are provided in Figure 6 for $A_{trans,3}$ = 3.5m and t_c = 100s. For this example, t_{EWF}=200s. Observe that while the 1st-order filter (for $t < \infty$) never actually reaches the 3.5-meter steady state value, the moving average reaches 3.5 meters in 100 seconds. Intuitively, a 100-second moving average of the SQM detection metrics will provide better transient SQM performance. Again, use of this type of smoothing does not impact steady state performance, since the SU MDEs already assume this filter implementation.

NEW DETECTION TEST: Δ^2- TEST

In order to further assist in the early detection of EWFs (without modifying the SQM2b correlator design), it is also desirable to make the detection metrics as sensitive as possible. It may not be sufficient to merely have exceeded the MDEs by an arbitrary amount. The maximum SQM test must be sufficiently large to detect the EWF before it causes the user error to exceed the MERR. A simple power operation performed on a sensitive detection metric may significantly increase this sensitivity even in the presence of noise and multipath.

Accordingly, the following detection "squared Δ-test" (Δ^2) was defined:

$$\frac{\left[\left(\Delta_{a,(\pm 0.075)} - \Delta_{a,ref} \right) - \left(\Delta_{nom,(\pm 0.075)} - \Delta_{nom,ref} \right) \right]^2}{MDE \left(\Delta^2_{(\pm 0.075),ref} \right)} \quad (7)$$

where $\left(\Delta_{a,(\pm 0.075)} - \Delta_{a,ref} \right)$ is the original (non-MDE-normalized) Δ-test of SQM2b without the nominal bias removed and uses correlator spacings, d=0.15T$_c$ and d_{ref}=0.1T$_c$. $MDE \left(\Delta^2_{(\pm 0.075), ref} \right)$ is the MDE associated with performing this squaring operation under nominal noise and multipath conditions. It was computed using the SU MDE data. In the above expression, *a* and *nom* represent the anomalous and nominal (filtered) waveforms, respectively. For LAAS, the reference correlator spacing, $ref = \pm 0.05T_c = 0.1T_c$.

Δ^2-test MDEs

The MDEs for the Δ^2-test are computed using the following equation

$$MDE = (a_3 \theta^3 + a_2 \theta^2 + a_1 \theta + a_0),$$

where θ is the elevation angle measured in degrees Table 1 lists the 3rd-order polynomial coefficients for the two (standard) Δ-tests and the Δ^2-test. The MDEs for the Δ^2-test are plotted below in Figure 7.

	a$_3$	a$_2$	a$_1$	a$_0$
$\Delta_{\pm 0.075, \pm 0.05}$	-5.5345e-009	1.6638e-006	-1.6604e-004	6.3401e-003
$\Delta_{\pm 0.1, \pm 0.05}$	-1.5115e-008	5.0539e-006	-3.7768e-004	1.3769e-002
$\Delta^2_{\pm 0.1, \pm 0.075}$	1.4044e-013	6.0462e-010	-9.3481e-008	3.6755e-006

Table 1 Polynomial Fit Coefficients for SQM2b Δ-tests and the Δ^2-test
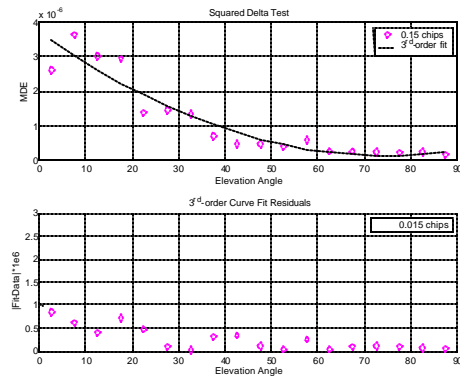

Figure 7 Curve fit and residuals for SQM2b Δ^2-tests

Recall that MDEs for the standard Δ-tests and ratio tests are computed according to

$$\text{MDE} = \left(k_{ffd} + k_{md} \right) \cdot \boldsymbol{s}_{test} \qquad (8)$$

where $k_{ffd} = 5.26$ yields a false alarm probability, P_{fa}, less than or equal to $1.5\mathrm{x}10^{-7}$, and $k_{md} = 3.09$ guarantees a missed-detection probability, P_{md}, no greater than 10^{-3}. σ_{test} represents the experimentally-measured standard deviation of the peak due to multipath and thermal noise. Accordingly, $\boldsymbol{s}_{test}$ assumes the distribution of those measurements is gaussian with a mean of zero.
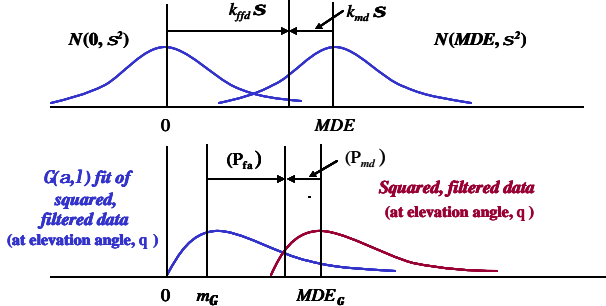
Figure 8 Computation of the "$\mathbf{D}^2$-Test" MDEs

The same procedure can compute a sigma for the Δ^2-test, but must also account for the fact that the distribution is chi-square—a special case of the 2-parameter gamma distribution.

The Δ^2-test data (for each satellite 5-degree elevation bin) is fit using the gamma distribution, and the threshold set from this curve fit corresponding to $P_{fa} = 1.5\mathrm{e}{-}7$. Next, the actual data for this bin is biased until 99.9% exceeds this threshold (i.e., the P_{md} equals $1.0\mathrm{e}{-}3$.). The amount of this bias equals MDE_G. (See Figure 8.) The MDE multiplier (inflation factor) is found from the ratio of the theoretical MDE computed by assuming a gaussian distribution, to the MDE obtained from the squared, filtered data (MDE_G). This is done for all 5-deg elevation angle bins from 0° to 90°.

Subsequently, Equation (8) can still compute the MDEs (using Δ^2-test measurements with the mean removed) provided a multiplication factor is applied to them to account for the difference in distribution assumptions. The MDE multiplier, y, is simply

$$y = \max\left\{ \left(0.0516\boldsymbol{q} + 0.3251 \right), 1.0 \right\} \qquad (9)$$

where θ is the satellite elevation angle (under consideration measured in degrees. plots this factor as a function of elevation angle. Note that although the elevation-dependent portion of Equation (9) may produce a multiplier less than unity for small elevation angles, the factor used in analysis was never less than unity.
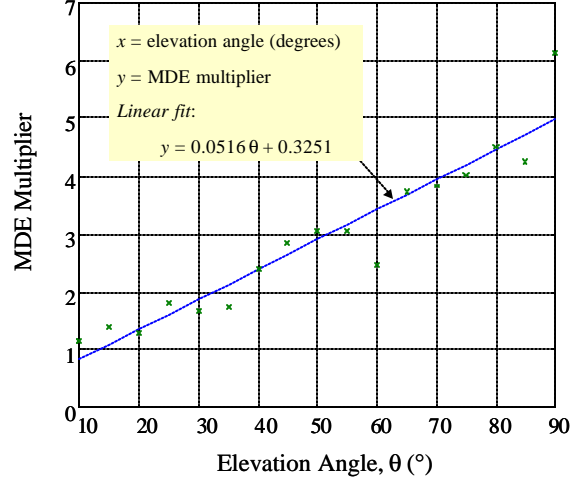

Figure 9 MDE Multiplier for Squared SQM Test

Error Sensitivity Issues

The Δ^2-test and higher-order power law tests (including exponential tests) *applied prior to any filtering operation* may improve transient SQM performance. Additionally, other tests (e.g., ratio tests) may prove viable candidates for these adaptations as well. It should be noted, however, that some sensitivity issues could arise with their actual implementation. These tests could become more sensitive to measurements errors—particularly those present in the nominal means, which must be pre-measured and stored offline for all the metrics. [4]

This can be seen using the following simple model of a Δ^2-test metric:

$$\left[\left(\Delta_{d1,d2} + \boldsymbol{e}_c \right) - \left(\overline{\Delta}_{d1,d2} + \boldsymbol{e}_{\overline{c}} \right) \right]^2 \qquad (10)$$

where

$\Delta_{d1,d2}$ is the difference of a delta-test at correlator spacing, d_χ, and reference spacing, d_{ref},

$\boldsymbol{e}_c$ is the (instantaneous) error in that detection measurement due to noise and multipath,

$\overline{\Delta}_{d1,d2}$ is the nominal mean of $\Delta_{d1,d2}$, and

$\boldsymbol{e}_{\overline{c}}$ is the error in $\overline{\Delta}_{d1,d2}$.

Manipulation of this equation and normalization of it by the appropriate MDE yields the following detection metric:

$$\frac{\left(\boldsymbol{c} - \overline{\boldsymbol{c}} \right)^2 + \left(\boldsymbol{e}_c - \boldsymbol{e}_{\overline{c}} \right)^2}{MDE_{c^2}} \qquad (11)$$

Note that all the previous (steady-state) EWF analyses (i.e., simulations), assumed e_c and $e_{\bar{c}}$ were zero. In that case the squared metric only increases the detectability margin of the (detectable) EWFs. In practice, however, the error terms may not be negligible. If they are not small, they may cause this detection metric to false alarm too frequently. Further experimentation and analysis using the real-time SQM monitor will be needed to more fully explore this issue [6].

SQM2 b: TRANSIENT PERFORMANCE

Steady state SQM analysis requires investigating the impact of all undetected points; however, the transient SQM analysis focuses on the detected points of SQM2b. Recall that the steady state analysis already showed that the undetected points (UDPs) corresponding to each respective elevation angle cause no hazardous errors at any time. Transient SQM analysis must verify that the detected points never introduce unacceptably large user PREs (before the monitor receiver detects them (minus 3 seconds)). In other words, it is necessary to analyze the effectiveness of SQM2b at detecting hazardous EWFs before $t = t_{HMI}+3s$.

Pursuing this idea, the analysis produced standard maximum PRE contour plots using both the 1st-order filter and the moving average filter to smooth the SQM metrics. The original 11 SQM2b detection tests were evaluated first [4],[6]. Only if unacceptable errors were found would it become necessary to implement the Δ^2-test. The contour plots assumed a satellite elevation angle of 90° and three available monitor receivers for both E-L and $\Delta\Delta$ correlators. This implies that they utilized the smallest MDEs for the detection of the EWFs from TM A, TM B, and TM C. Accordingly this analysis examines the maximum number of *detected points* in the EWF threat spaces.

The plots for each case are given below. Here, the maximum PREs correspond to the maximum differential (EWF) tracking errors experienced by the airborne users at time, $t=t_{detect}$, whenever SQM2b did not detect the EWF within the allotted TTA. Otherwise, no transient EWF error would occur, hence no error contour appears. (As was true for the steady state contour plots, a thick, heavily shaded contour is plotted wherever the 90°-MERR threshold is crossed.) For $TTA_{lgf}=3s$, Figures 10 through 15 plot the 1st-order filter cases and Figures 16 through 21 plot the moving average filter results.

Observe that for almost all cases, no contours within any of the regions for both E-L and $\Delta\Delta$ users are above the (most conservative) 90°-MERR. In fact, for $TTA_{lgf} = 3s$, only the $\Delta\Delta$ receivers suffered any unacceptably large transient EWF PREs. (Results from $TTA_{lgf} = 0s$ are provided in [4].) TM C, however, is the only case for which there were unacceptable transient PREs—for a few ?? configurations—with $TTA_{lgf} = 3s$. This implies that the Δ^2-test may be required to protect these users under transient TM C EWF conditions.

Using the Δ^2-test, a single maximum PRE contour plot for the ??-receiver users subjected to TM C EWFs was generated and is provided in Figure 22 and Figure 23. The nominal MDEs for the Δ^2-test were computed from the SU MDE data for all elevation angles as detailed in [3] and [4]. (Including the inflation factor, the nominal 90° elevation angle MDE(Δ^2) for this test was computed as 7.521e-7.) The analysis used the nominal MDE, a moving average filter assumption, and a $TTA_{lgf} = 3s$. The results indicate that SQM2b, with the inclusion of the Δ^2-test, adequately protects these users against the hazardous transient TM C EWFs. The plot summarizes the maximum differential PRE results for all elevation angles between 0° and 90°; it shows only the "notch" region of the $\Delta\Delta$ Region 2 user configuration space.

$\mathbf{D}^2$-TEST PERFORMANCE VALIDATION

The relative advantage of the Δ^2-test was demonstrated using a real-time SQM prototype capable of generating 2OS waveforms on the C/A code. The prototype generated an analog and digital failure EWF corresponding to Fault Case 5 described in [6] (f_d=10MHz, σ=0.8Mnep/sec, and Δ=9nsec). The validation compared the detection times, t_{detect}, for the original 11 SQM2b detection tests to those of the Δ^2-test.

Two sets of 10 trials were each run at high (48dB-Hz) and low (32dB-Hz) C/N_0. (N_0 was set at –155dBm/Hz.) These two sets of trials attempted to simulate a 60° and a 5°-elevation angle SV, respectively. For these trials the minimum MDE multiplier, y, of 2—a more conservative value—was used for the 5° case, to ensure no false alarms occurred. (Since y is still greater at larger elevation angles, and the corresponding MERRs are smaller, the analysis still represents the worst case expected performance.) Figure 24 shows time traces from a single trial (at 48dB-Hz) and Table 2 summarizes the results from all 20 trials. The table shows that the Δ^2-test consistently detects the anomaly significantly faster.
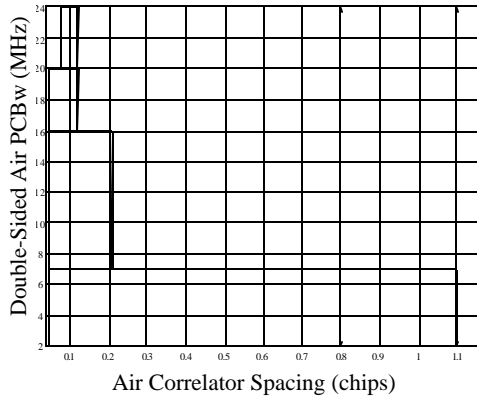
1st-Order Filter Results: (TTA$_{lgf}$ = 3s)
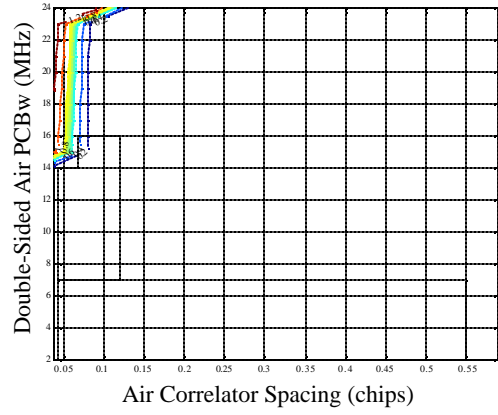

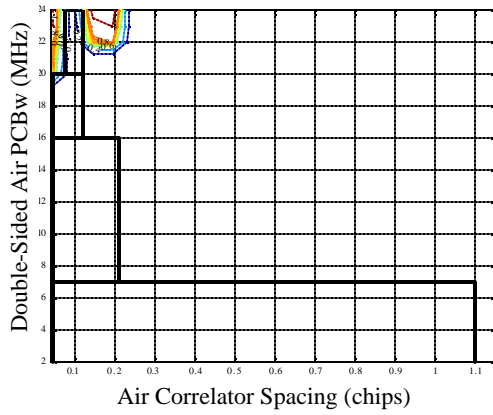**Figure 10 E-L - TM A**

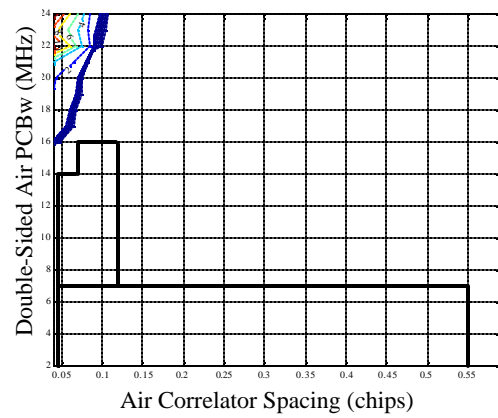**Figure 13 DD - TM A**

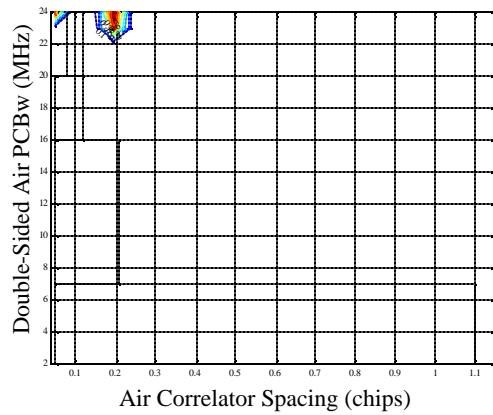**Figure 11 E-L - TM B**

Figure 14 DD - TM B
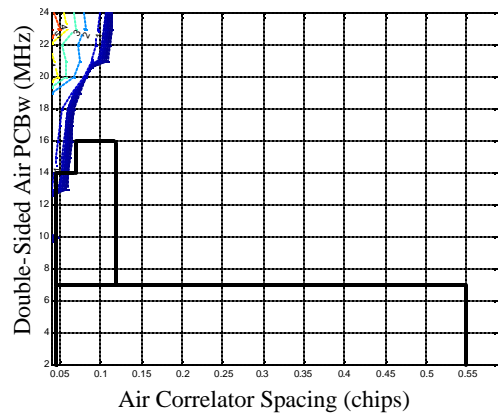

Figure 12 E-L – TM C

Figure 15 DD - TM C
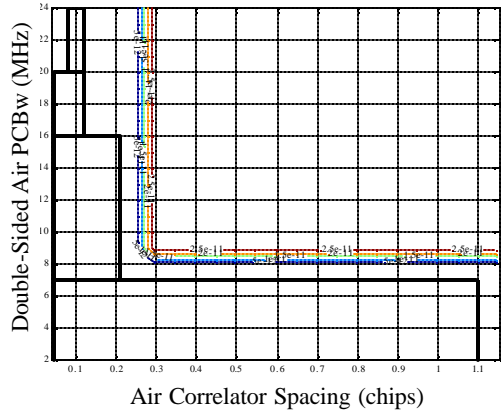
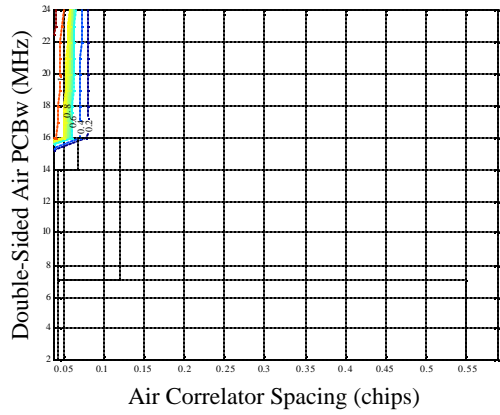*Moving Average Filter Results: (TTA$_{lgf}$ = 3s)*
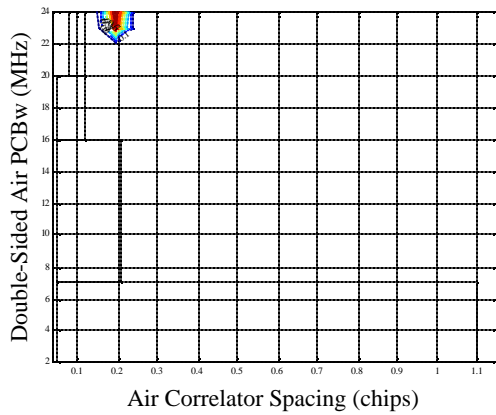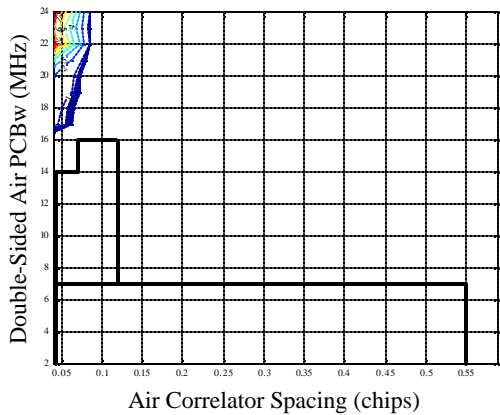

Figure 16 E-L - TM A

Figure 19 ? ? - TM A

Figure 17 E-L - TM B

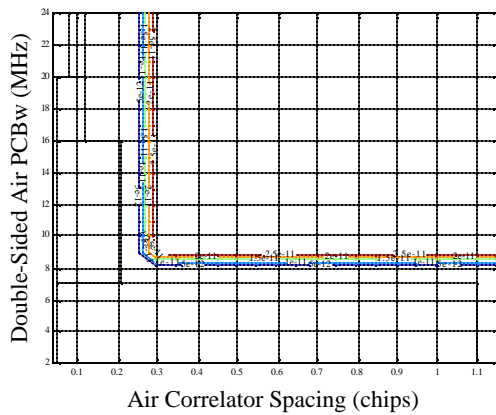**Figure 20 ? ? - TM B**
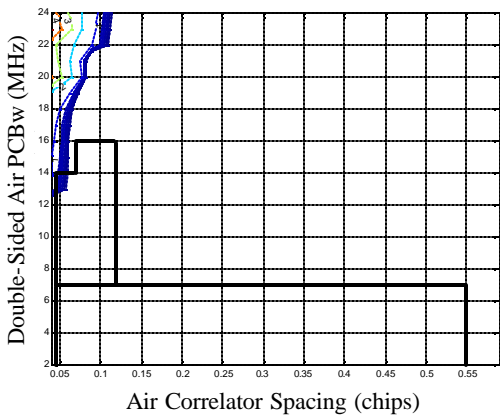

Figure 18 E-L - TM C
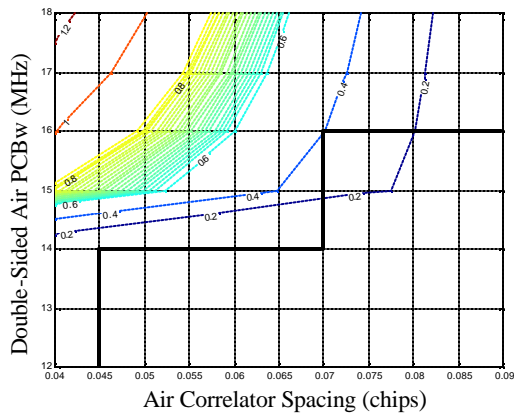

Figure 21 ? ? - TM C

Figure 22 DD - Correlators – TM C (with D²-test) – 1ˢᵗ-order Filter, Notch Region Shown Only (All Other PREs in Design Space are Smaller.)
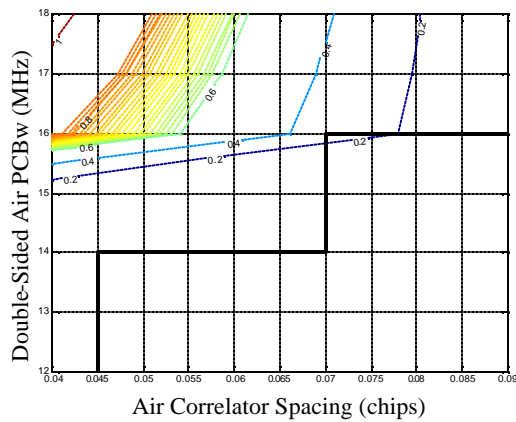

Figure 23 DD - Correlators – TM C (with D²-test) – Moving Average Filter, Notch Region Shown Only (All Other PREs in Design Space are Smaller.)
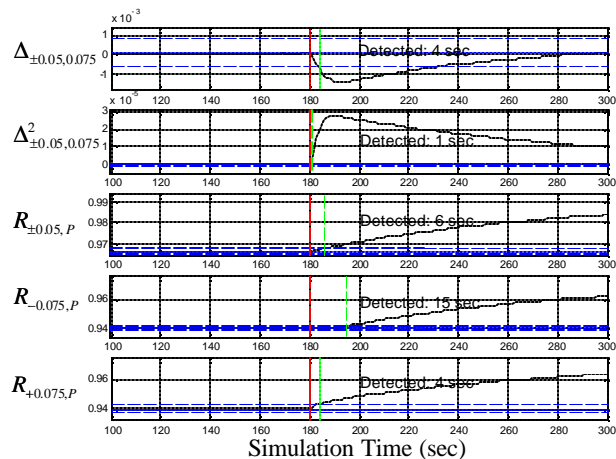

Figure 24 Transient Response Time Traces of Several SQM2b Detection Test Including the D²-Test.

t_{detect} (sec) for Fault Case No. 5 (f_d=10MHz, σ=0.8Mnep/sec, Δ=0.9T$_c$) Min, Mean, and Max from 10 Trials						
	C/N₀=32dB-Hz (θ=5°)			C/N₀=48dB-Hz (θ=60°)		
Detection Test	Min	Mean	Max	Min	Mean	Max
$\Delta_{\pm0.05,0.075}$	–––	–––	–––	3	4.1	5
$\Delta_{\pm0.05,0.1}$	–––	–––	–––	5	6.1	7
$R_{\pm0.05,P}$	26	27.2	32	5	5.8	7
$R_{\pm0.075,P}$	34	35.2	37	7	7.1	8
$R_{\pm0.1,P}$	44	45.3	47	7	7.2	8
$R_{-0.05,P}$	31	32.9	37	10	11.7	13
$R_{-0.075,P}$	30	33.1	36	14	14.7	16
$R_{-0.1,P}$	29	32.1	35	14	15.3	17
$R_{+0.05,P}$	20	22.2	27	2	3.0	4
$R_{+0.075,P}$	20	41.0	43	4	4.1	5
$R_{+0.1,P}$	20	76.7	82	4	4.7	6
$\Delta^2_{\pm0.05,0.075}$	2	2.5	4	1	1.1	2

Table 2 10-Trial Summary of Detection Times (in Seconds) for Original 11 SQM2b Detection tests and D²-test.

CONCLUSION

Previous SQM analysis studies dealt only with the steady-state performance of the evil waveform monitor. Without additional processing, the monitor design SQM2b—using only the 11 original detection tests—cannot protect all ΔΔ users when the LAAS time-to-alarm requirement is considered. More specifically, the transient responses of the filters might prevent the original SQM2b detection tests from mitigating the EWFs before they cause HMI for some airborne users. The response time of the detection tests could be reduced without penalty by using a 100-second moving average to smooth the test measurements instead of a first-order filter. However, this modification made only marginal improvement in transient performance of the original SQM2b tests.

As a result, the Δ²-test was introduced and analyzed. The analysis found that the addition of this single test made SQM2b capable of protecting all airborne users against EWFs within the 6-second time-to-alarm. This test was

experimentally verified using a real-time SQM prototype. The Δ^2-test is capable of detecting hazardous EWFs significantly faster than the 11 original tests.

REFERENCES

[1] Enge, P. K., Phelts, R. E., Mitelman, A. M., "Detecting Anomalous signals from GPS Satellites," ICAO, GNSS/P, Toulouse, France, 1999.

[2] Edgar, C., Czopek, F., Barker, B., "A Co-operative Anomaly Resolution on PRN-19," *Proceedings of the 2000 13th International Technical Meeting of the Satellite Division of the Institute of Navigation*, *ION GPS-2000*. Proceedings of ION GPS 2000, v 2, pp. 2269-271.

[3] Phelts, R. E., Akos, D. M., Enge, P. K., "Robust Signal Quality Monitoring and Detection of Evil Waveforms," *Proceedings of the 13th International Technical Meeting of the Satellite Division of the Institute of Navigation*, ION-GPS-2000, pp. 1180-1190.

[4] Phelts, R. E. "Multicorrelator Techniques for Robust Mitigation of Threats to GPS Signal Quality," Ph.D. Thesis, Stanford University, Stanford, CA, 2001.

[5] Macabiau, C., Chatre, E., "Impact of Evil Waveforms on GBAS Performance," *Position Location and Navigation Symposium*, IEEE PLANS, pp. 22-9, 2000.

[6] Mitelman, Alexander M., Phelts, R. E., Akos, D. M., Pullen, Samuel P., Enge, P. K., "A Real-Time Signal Quality Monitor for GPS Augmentation Systems," *Proceedings of the 13th International Technical Meeting of the Satellite Division of the Institute of Navigation*, ION-GPS-2000, pp. 177-84.

[7] Garin, L., van Diggelen, F., Rousseau J-M., "Strobe and Edge Correlator Multipath Mitigation for Code," *Proceedings of the 1996 11th International Technical Meeting of the Satellite Division of the Institute of Navigation*, *ION GPS-98*, Proceedings of ION GPS 1996, 1996 v 1, pp. 657-64.

[8] Garin, L., Rousseau, J.-M., "Enhanced Strobe Correlator Multipath Mitigation for Code and Carrier," *Proceedings of the 10th International Technical Meeting of the Satellite Division of the Institute of Navigation, ION-GPS-97*, Part 1(of 2), Proceedings of ION-GPS, 1997 v l. 1, pp. 559-68.

[9] McGraw, G. A., Braasch, M. S., "GNSS Multipath Mitigation Using Gated and High Resolution Correlator Concepts," *Proceedings of the 12th-Internatinal Technical Meeting of the Satellite Division of the Institute of Navigation*, ," ION GPS-99, pp. 333-42, 1999.

[10] *Specification: Performance Type One Local Area Augmentation System Ground Facility*. U.S. Federal Aviation Administration, Washington, D.C., FAA-E-2937, Sept., 21, 1999.